Calculation of the Ionization Constant of H_2O to 2,273 K and 500 MPa

Calculations of the ionization constant of H_2O are presented for densities ranging from those of subcritical water to those of supercritical steam. A recently-proposed semicontinuum model is used to calculate the standard-state hydration properties for the ions, H_3O^+, and OH^- (Tanger and Pitzer, 1989). Calculated ionization constants are in good agreement with reported measurements at pressures from vapor-liquid saturation to 500 MPa and temperatures from 273 to 1,073 K. These measurements cover H_2O densities ranging from ~1,000 to 450 kg · m^{-3}. At H_2O densities less than 400 kg · m^{-3}, our calculated ionization constants should be more reliable than those obtained from the commonly-used equation of Marshall and Franck (1981).

John C. Tanger IV
Kenneth S. Pitzer
Department of Chemistry
and Lawrence Berkeley Laboratory
University of California
Berkeley, CA 94720

Introduction

Methods for calculating equilibrium constants for aqueous ionic equilibria over very wide ranges of pressure and temperature are a prerequisite for reliable computer simulation of chemical reactions in both natural and industrial aqueous fluids. These computer simulations are valuable investigative tools for researchers in such areas as industrial boiler and steam turbine chemistry, geothermal energy, steam treatment of hazardous wastes, and hydrothermal synthesis of solids. The ionization of H_2O is one of the most important reactions in these high-temperature fluids, and the ionization constant, K_w, has been measured to very high temperatures and pressures. (See Marshall and Franck, 1981, for review of measurements.) Previously-proposed equations for K_w presented by Marshall and Franck (1981) (MF81) and Pitzer (1982) (P82) can be applied reliably only in separate solvent density regions: i.e., $\rho > 400$ kg · m^{-3} for MF81 and $\rho < 100$ kg · m^{-3} for P82.

In this paper, a simple thermodynamic cycle and a semicontinuum model for ionic hydration (Tanger and Pitzer, 1989) are used to calculate log K_w over the full range of solvent densities at temperatures from 273 to 2,273 K and pressures up to 500 MPa. Our calculated values of log K_w are in good agreement with measured values as well as with corresponding values obtained from the MF81 and the P82 equations within their respective validity regions. Calculation procedures and estimated uncertainties are discussed, and tabulated log K_w values are provided.

Calculation of Log K_w

The change in the Gibbs free energy for the ionization of H_2O, ΔG_w, can be obtained from the following thermodynamic cycle:

Cycle I

$$2H_2O_{(g,T)} \xrightarrow{2} H_3O^+_{(g,T)} + OH^-_{(g,T)}$$

$$1 \uparrow \qquad\qquad \downarrow 3$$

$$2H_2O_{(fl,P,T)} \xrightarrow[4]{} H_3O^+_{(aq,P,T)} + OH^-_{(aq,P,T)}$$

where g, fl, and aq represent standard states of hypothetical ideal gas at 1 bar, pure fluid, and hypothetical one molal ideal solution, respectively. For step 1 of Cycle I, ΔG_1 accounts for the free energy change resulting from the change in the solvent standard state ($fl \rightarrow g$). Values of ΔG_1 are obtained from

$$\Delta G_1 = \Delta_f G_{H_2O(g,T)} - \Delta_f G_{H_2O(fl,P,T)}$$

where $\Delta_f G$ stands for the Gibbs free energy of formation. In our calculations, we used values of $\Delta_f G_{H_2O(g,T)}$ and $\Delta_f G_{H_2O(fl,P_r,T_r)}$ from Chase et al. (1985), where P_r and T_r denote the reference pressure and temperature of 0.1 MPa and 298 K, and we evaluated $[\Delta_f G_{H_2O(fl,P,T)}]$ using the equation of state for pure H_2O given by Haar et al. (1984).

For step 2 of Cycle I, ΔG_2 represents the free energy change for the bimolecular ionization of ideal gas H_2O. Values of ΔG_2 and log K_2 can be calculated using the $\Delta_f G$ values for $H_2O_{(g)}$, $H_3O^+_{(g)}$, and $OH^-_{(g)}$ given by Chase et al. (1985). At temperatures from 273 to 2,273 K, these values of log K_2 can be approximated within ±0.03 base ten log units by the van't Hoff equation, $\ln K_2 = -\Delta H_2/RT + \Delta S_2/R$, where ΔH_2 and ΔS_2 represent the

Correspondence concerning this paper should be addressed to J. C. Tanger IV, who is currently at Chemical Thermodynamics Division, Center for Chemical Physics, National Institute of Standards and Technology, Gaithersburg, MD 20899.

changes in the standard-state enthalpy and entropy, respectively, for step 2 at 298 K from Chase et al. (1985). In our calculations, we used this van't Hoff equation to obtain log K_2.

For step 3 of Cycle I, ΔG_3 represents the Gibbs free energy of hydration, $\Delta_h G$, for $H_3O^+ + OH^-$. Values of $\Delta_h G$ are calculated using a semicontinuum model, as will be discussed later. Finally, ΔG_4 corresponds to ΔG_w. Step 4 is represented as a bimolecular process because the first hydration of the proton is complete under all conditions of practical interest (Giguere, 1979; Pitzer, 1982). It follows from Cycle I that

$$\log K_w = [-2\Delta G_1/RT - \Delta G_2/RT - \Delta_h G/RT]/\ln(10). \quad (1)$$

The equation from the semicontinuum model (Tanger and Pitzer, 1989) for $\Delta_h G$ of the kth, 1:1 aqueous electrolyte (e.g., $H_3O^+ + OH^-$) is written as

$$\Delta_h G/\mathrm{RT} = -\sum_{\text{ions}} \ln\left\{1 + \sum_{n=1}^{n=6}\left[f^n_{H_2O} \exp(-nP\bar{V}^*_{H_2O}/\mathrm{RT}) \prod_{j=1}^{j=n} K_j\right]\right\} + \frac{2\eta}{TR^*_k}\left(\frac{1}{\epsilon} - 1\right) + 2\ln\left(\frac{\mathrm{RT}\rho}{1{,}000}\right), \quad (2)$$

where f_{H_2O}, ϵ, and ρ represent the fugacity, dielectric constant and density of pure H_2O, respectively; n stands for the number of inner shell H_2O molecules hydrating the ion (n = 1 to 6); $\bar{V}^*_{H_2O}$ denotes the effective molal volume increment per inner shell H_2O molecule of hydration; $\eta = 8.3549 \times 10^{-6}$ m · K; R^*_k represents the effective electrostatic Born radius for the kth electrolyte; and K_j denotes the equilibrium constant for the successive ion hydration reaction,

$$\text{ion}(H_2O)_{j-1} + H_2O = \text{ion}(H_2O)_j.$$

In our calculations using Eq. 2, we obtain values for f_{H_2O} and ρ from the equation of Haar et al. (1984). Dielectric constant values are calculated using the equation of Uematsu and Franck (1980) for most liquid-like H_2O densities, and the equation of Pitzer (1983) is used at lower densities. The K_j equilibrium constants are calculated using the experimental values of ΔH_j and ΔS_j given in Table 1 and the van't Hoff expression, $\ln K_j = \Delta S_j/R - \Delta H_j/RT$.

The semicontinuum approach treats the solvent in the region nearest the ion, as discrete molecules and outside this region the solvent is treated as a continuum. The last term on the righthand side of Eq. 2 accounts for the change in standard states in the ion hydration process ($g \rightarrow aq$). The first term in Eq. 2 represents the inner shell contribution which accounts for contributions to $\Delta_h G$ from an inner shell containing up to six H_2O molecules. The second term in Eq. 2 represents the outer shell contribution, and we use the Born equation to account for these long-range, electrostatic ion-solvent interactions.

Table 1. Experimental Enthalpy and Entropy Changes for Successive Hydration of H_3O^+ and OH^- Ions*

Ion, j	1	2	3	4	5	6
	$-\Delta H_j$(kJ · mol^{-1})					
H_3O^+	132.2	81.6	74.9	53.1	48.5	44.8
OH^-	104.6	74.9	63.2	59.4	59.0	(56.1)**
	$-\Delta S_j$(J · mol^{-1} · K^{-1})					
H_3O^+	101.7	90.8	118.8	97.9	104.6	109.2
OH^-	87.0	88.7	103.8	123.4	138.9	(138.9)**

*Data from Lau et al. (1982), Arshadi and Kebarle (1970), and Payzant et al. (1971).
**Parentheses indicate our estimates.

The effective radius for the kth aqueous electrolyte is defined in terms of the corresponding radii of its cations and anions as $R^*_k \equiv 2(\nu_+ Z_+/R^*_+ + \nu_- Z_-/R^*_-)^{-1}$, where ν stands for a stoichiometric coefficient and Z denotes ionic charge. R^*_+ or R^*_- represents the effective radius of a spherical cavity in the dielectric continuum which contains the inner shell region. In our model, the R^* parameter is taken to be independent of pressure.

The basic equation for the inner shell contribution is $\Delta_h G$ (inner shell)/RT = $\ln(1 + \Sigma_{n-1}^{n-6} X_n/X_o)$, where X denotes mole fraction, and the subscripts n and o denote a hydrated species with n H_2O and the anhydrous gaseous solute species, respectively (Pitzer, 1982). General thermodynamic relations permit expression of X_n/X_o as $f^n_{H_2O}(\phi_o/\phi_n)\Pi_{j-1}^{j-n} K_j$, where ϕ represents a fugacity coefficient. By defining $\bar{V}^*_{H_2O}$ as equal to $(\bar{V}_n - \bar{V}_o)/n$ and by assuming that $\bar{V}^*_{H_2O}$ is independent of pressure, it can be shown that ϕ_o/ϕ_n is equal to $\exp(-nP\bar{V}^*_{H_2O}/\mathrm{RT})$.

The model parameters $\bar{V}^*_{H_2O}$ and R^*_k in Eq. 2 are described by empirical temperature functions (Tanger and Pitzer, 1989) given by

$$\bar{V}^*_{H_2O} = d_1 + d_2 t + d_3/(d_4 + t^3) + d_5 r_x^3, \quad (3)$$

and

$$R^*_k = R^*_{k,T_r}\tau, \quad (4)$$

where

$$\tau = b_1 + b_2 T + b_3/T^2 \quad \text{for} \quad T > 498\ \text{K} \quad (5a)$$

and

$$\tau = b_4 + b_5 T + b_6 T^2 \quad \text{for} \quad 273 \text{ to } 498\ \text{K} \quad (5b)$$

and where d_1 through d_5 and b_1 through b_6 denote ion-independent empirical constants, r_x stands for the octahedral crystallographic (Pauling's) radius of the ion, t represents °C, T_r denotes 298 K, and τ = 1 at 298 K. Equations 3–5 are consistent with a more open configuration of inner shell H_2O molecules produced by increases in temperature or ion size. In our present calculations with Eq. 3, we used the values for d_1 through d_5 given in Table 2, and we assumed that the r_x of OH^- equals the r_x for O^{-2} (0.140 nm; Arhens, 1952) which are consistent procedures with our previous calculations (Tanger and Pitzer, 1989). At this point we need to obtain values of r_x for H_3O^+, R^*_{k,T_r} for $H_3O^+ + OH^-$ and τ in order to calculate log K_w using Eqs. 1–4.

"Best fit" values of τ (see Figure 1) and R^*_{k,T_r} were obtained using Eqs. 1–4 and the log K_w experimental data of Sweeton et al. (1974) (see Table 3) and Quist (1970) (see Figures 2 and 3). The upper and lower "best-fit" τ values for Quist's data shown in Figure 1 are the maximum and minimum values, respectively,

Table 2. Coefficients for Eqs. 3, 5a, and 5b

n	d_n*	b_n**
1	17.84	0.9642
2	7.583×10^{-4}	3.0738×10^{-4}
3	-3.718×10^{7}	-4.9203×10^{3}
4	1.064×10^{7}	0.7417
5	1.343	1.0923×10^{-3}
6		-7.5825×10^{-7}

*From Tanger and Pitzer (1989) for $10^{-6} \times \bar{V}^*_{H_2O}$ in $m^3 \cdot mol^{-1}$.
**This study.

for the indicated temperature. Because of the ambiguities which arise in selection of appropriate Pauling's radii for OH^- and H_3O^+, we fixed $r_x(OH^-)$ as given above and we treated $r_x(H_3O^+)$ as an adjustable parameter. The "best-fit" τ values obtained from the data of Sweeton et al. (1974), together with Eqs. 1–4 and the high-pressure log K_w measurements of Kryukov et al. (1980) (see Figure 4), permitted determination of a "best-fit" value for $r_x(H_3O^+)$. The calculations described above yielded "best-fit" values for $R^*_{k,T_r}(H_3O^+ + OH^-)$ and $r_x(H_3O^+)$ of 0.26549 nm and 0.155 nm, respectively.

Ion additivity relations require that the temperature function τ should be independent of the aqueous electrolyte (or ion). The uncertainties in the experimental values for ΔH_j and ΔS_j (Eq. 2 Table 1), however, translate into rather large uncertainties in calculated "best-fit" τ values. As demonstrated previously (Tanger and Pitzer, 1989), the τ function can be taken as electrolyte-independent when these experimental uncertainties are considered. Nevertheless, unambiguous determination of a unique τ function is not straightforward. Consequently, values of b_1 through b_6 used in our present calculations and given in Table 2 were obtained by regression of the "best-fit" τ values (Figure 1) using Eqs. 5a–b. The solid curve in Figure 1 represents Eqs. 5a–b and Table 2.

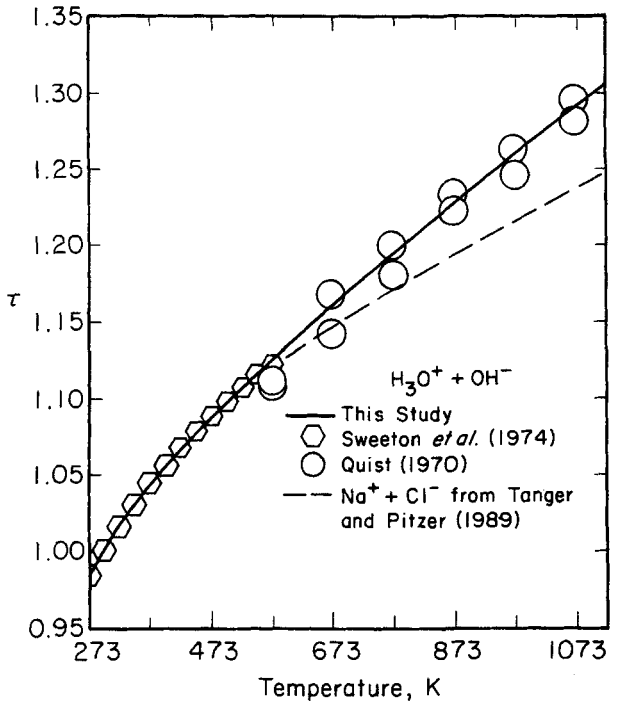

Figure 1. Eqs. 5a and b and Table 2 (solid curve) for the semicontinuum model parameter, τ, as a function of temperature.

Symbols denote "best-fit" values of τ for $H_3O^+ + OH^-$. Dashed curve represents regression results reported by Tanger and Pitzer (1989) which were obtained using Eqs. 5a–b and "best-fit" τ values for $Na^+ + Cl^-$.

Table 3. Comparison of Log K_w (Base 10) Calculated Using Eqs. 1–5 with Experimental Values for Coexisting Liquid at Saturated Vapor Pressure

T, K*	log K_w**	δ log K_w†	T, K	log K_w	δ log K_w
273	−14.961	0.020	448	−11.457	0.016
298	−13.994	0.001	473	−11.310	0.008
323	−13.256	−0.016	498	−11.206	−0.016
348	−12.689	−0.020	523	−11.199	0.003
373	−12.251	−0.013	548	−11.265	0.041
398	−11.914	0.000	573	−11.404	0.103
423	−11.654	0.012			

*Exact temperatures for values given without a decimal point are higher by 0.15 K.
**Calculated in this study.
†Experimental values reported by Sweeton et al. (1974) minus corresponding values obtained in this study.

The dashed curve in Figure 1 denotes our previous regression results with Eqs. 5a–b for $Na^+ + Cl^-$. The τ values for $Na^+ + Cl^-$ are representative of those for the alkali metal halide and the alkali metal hydroxide electrolytes. As can be seen in Figure 1, the difference between τ values for $H_3O^+ + OH^-$ and $Na^+ + Cl^-$ increases steadily to rather large values as temperature increases above 573 K. These differences, however, are within the expected uncertainties for "best-fit" τ values (Tanger and Pitzer, 1989). In addition, the sensitivity of our model to the value of τ decreases systematically with increasing temperature because the dielectric constant decreases toward unity. If we use the τ values for $Na^+ + Cl^-$ in place of those for $H_3O^+ + OH^-$, the maximum change in our calculated log K_w values is only 0.8 log units at 500 MPa and 1,273 K for temperatures from 273 to

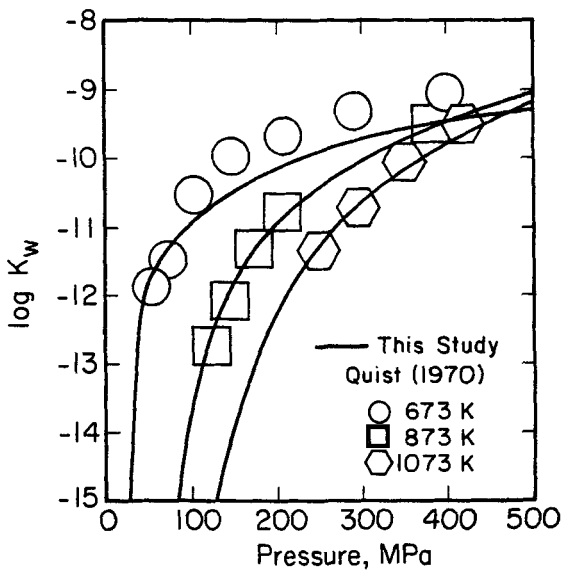

Figure 2. Calculated values for log K_w from Eqs. 1–5 (curves) vs. experimental values (symbols) along selected isotherms as a function of pressure.

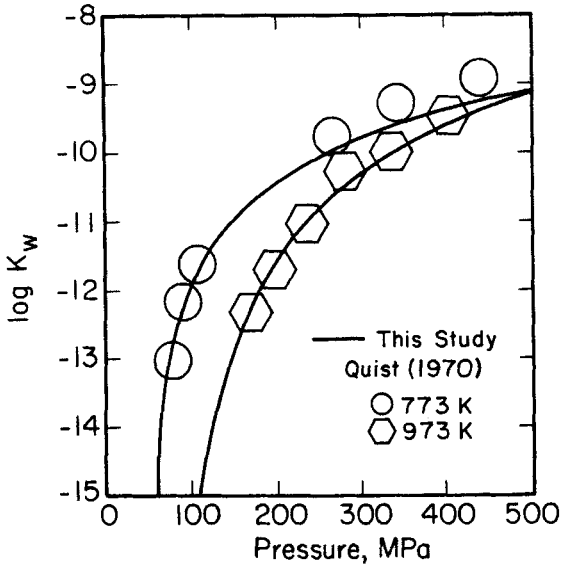

Figure 3. Calculated values for log K_w from Eqs. 1–5 (curves) vs. experimental values (symbols) along selected isotherms as a function of pressure.

2,273 K and all pressures up to 500 MPa. Consequently, the present calculations do lend additional support to the proposed ion-independence of the τ function.

Experimental Data vs. Other Equations

Our calculated log K_w values at vapor-liquid saturation pressure are given in Table 3 along with corresponding differences, δ log K_w, with respect to measured values given by Sweeton et al. (1974). These differences, δ log K_w, are slightly larger than the reported experimental uncertainties. It is possible, however, to smoothly fit the "best-fit" τ values obtained from Sweeton et al. (1974) more closely than we have done using Eqs. 5a–b and Table 2. Nevertheless, Eqs. 5a–b and Table 2 provide sufficient accuracy for our present purposes. It should be noted that predicted values for log K_w from the model of Tanger and Helgeson (1988) agree with the measurements of Sweeton et al. (1974) within experimental uncertainties. Calculated log K_w values from the MF81 equation at vapor-liquid saturation pressure are also within these experimental uncertainties except at 573 K.

Calculated values of log K_w obtained using Eqs. 1–5 can be compared with high-pressure measurements in Figures 2–4. With respect to the experimental values of log K_w from Quist (1970) represented in Figures 2 and 3, the MF81 equation yields somewhat better agreement than our values at 673 and 773 K. However, Quist points out that his values are especially uncertain at 673 K and the higher pressures. In contrast, our values are in better agreement overall with Quist's measured values than those obtained from the MF81 equation at 873 K, 973 K, and 1,073 K. Our Eqs. 1–5, as well as the MF81 equation, agree with the measured values of log K_w within the estimated experimental uncertainty of 0.3 to 0.5 log units (Quist, 1970). The above comparisons suggest that, for H_2O densities >450 kg · m^{-3}, our model is as reliable os the MF81 equation for temperatures down to ~573 K.

With respect to the pressures and temperatures considered in Figure 4, calculated values of log K_w reported by Marshall and Franck (1981) and Tanger and Helgeson (1988) are generally in better agreement with corresponding experimental values than our results. It should be noted, however, that, for pressures from 300 to 500 MPa, the other two equations mentioned above commonly do not agree with measured log K_w values within the experimental uncertainties reported by Kryukov et al. (1980). Differences between log K_w from our model and corresponding measured values (Figure 4) are usually three times larger than the reported experimental uncertainties. In the Appendix, we demonstrate that a simple revision of our conceptual model for the $\bar{V}^*_{H_2O}$ parameter in Eq. 2 permits closer description of the high-pressure experimental data shown in Figure 4. However, we have used Eq. 3 to represent $\bar{V}^*_{H_2O}$ in all other calculations presented here, because it provides sufficient accuracy for our present purposes.

In Figure 5, our calculated values of log K_w can be compared with those calculated by Pitzer (1982) and Klots (1984) at steam conditions for H_2O. The agreement of our model with the log K_w values for the vapor at the saturation pressure reported by Klots (1984) seems reasonable to us in light of the more approximate nature of his "liquid-drop" model. At low-pressure steam conditions, H_2O is nearly an ideal gas and its dielectric constant is very close to unity. Our Eq. 2 reduces to the P82 equation at these steam conditions. Consequently, log K_w values obtained from the present model are close to those obtained previously (Pitzer, 1982) at pressures of 10 MPa or less (Figure 5). The agreement with these earlier values at 0.1 MPa is within ±0.2 log units. The agreement at 0.1 MPa would be exact except that we took the heat capacities of successive ion hydration reac-

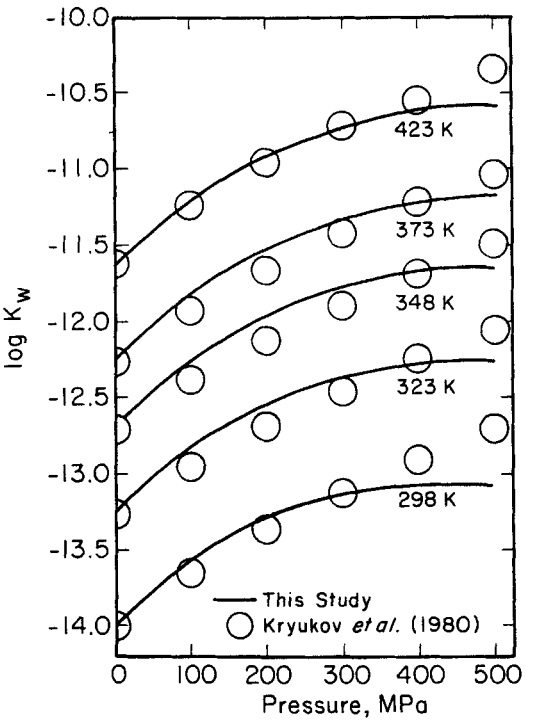

Figure 4. Calculated values for log K_w from Eqs. 1–5 (curves) vs. experimental values (symbols) along selected isotherms as a function of pressure.

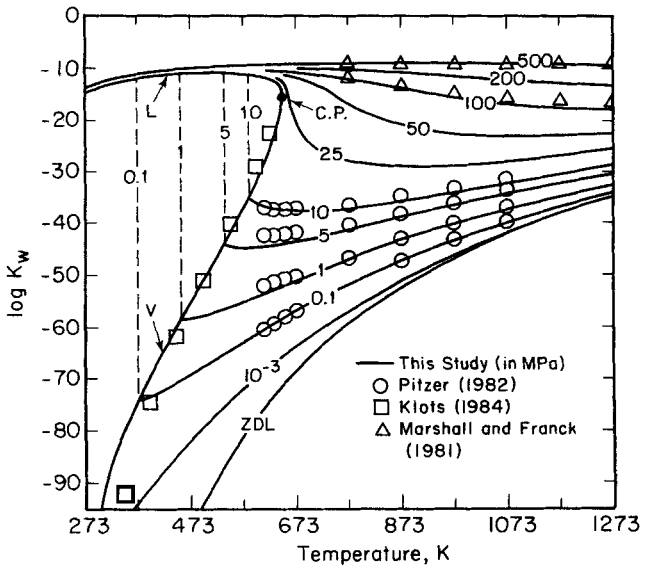

Figure 5. Calculated values for log K_w from Eqs. 1–5 (curves) vs. those calculated values from other equations (symbols) along selected isobars as a function of temperature.

ZDL stands for zero density limit (see Figure 6). Dashed isobars connect log K_w values for coexisting liquid and vapor.

tions as equal to zero, while a value of 3.5 R was used in the earlier study.

Discussion

It has been demonstrated previously (Pitzer, 1982) that the MF81 equation is not reliable at pressures and temperatures where the density of H_2O is less than ~400 kg · m^{-3}. In contrast, Eqs. 1–5 are expected to be reasonably accurate at $\rho \leq 400$ kg · m^{-3}. In addition, for $\rho > 400$ kg · m^{-3} and temperatures down to ~573 K, log K_w values from Eqs. 1–5 should be as reliable as those obtained from the MF81 equation. Consequently, we have prepared tabulated log K_w values from our model for the pressure-temperature regions where the reliability of our values is equal to or greater than those given by Marshall and Franck (1981). Our calculated log K_w values at pressures and temperatures in the critical region which are of special interest to the steam power industry are given in Tables 4 and 5 (see also Supplementary Material).

Extension of our calculations to 2,273 K, as shown in Figure 6, is permitted by a simple and nearly linear extrapolation of $\bar{V}^*_{H_2O}$ and τ (Eqs. 3 and 5a) to 2,273 K. As can be seen in Figure 6, extrapolation of our model yields reasonable high-temperature extensions of log K_w isobars to 2,273 K. In the limit $\rho \rightarrow 0$ (or $P \rightarrow 0$), Eqs. 1–5 for log K_w approach log K_2 − 2 log (M_w/1,000), where M_w represents the mole weight of H_2O. The zero-density-limit (ZDL) log K_w values are almost exactly linear when plotted vs. $1/T$ as shown in Figure 6 by the line labeled ZDL. It should be noted that the error in the MF81 equation becomes quite large at low densities because log K_w values from this equation approach minus infinity instead of the correct zero density limit.

The major sources of uncertainties in our calculated values of log K_w (Eq. 1) arise from $\Delta G_2/[RT \ln (10)]$, (= log K_2), and $\Delta_h G/[RT \ln (10)]$, (= log K_h). Uncertainties in calculated values of ΔG_1 should be relatively trivial because the fluid-state properties of pure H_2O are well known, as discussed previously. We also investigated other possible ionization and decomposition reactions for H_2O and found that the concentrations of other likely ionization products (e.g., O^-, H^-, O^+, H^+, OH^+) are negligible compared to H_3O^+ and OH^-. As temperatures approach 2,000 K, decomposition of H_2O to H_2 and O_2 produces higher concentrations of H_2 and O_2 relative to H_3O^+ and OH^-. However, this decomposition does not significantly affect the activity of H_2O, because the concentrations of H_2 and O_2 are still quite small.

The most significant uncertainty contributions to ΔG_2 stem from the enthalpies of formation for H_3O^+ and OH^- at 298 K. Adding the uncertainties for these two quantities as given by Chase et al. (1985) and then dividing by R(298) ln (10) gives a temperature-independent uncertainty for log K_2 of 2.9 log units. Although log K_2 could be in error by this amount, the uncertainties in our model are much smaller than this at 273 to 1,073 K and $\rho > 400$ kg · m^{-3}. The empirical parameters in our model allow compensation for possible errors in log K_2 and log K_h over the temperature and density range of the experimental data for log K_w. Nevertheless, as density approaches zero, the uncertainties in log K_w from our model approach the corresponding uncertainties for log K_2.

Table 4. Negative Log (Base 10) of Dissociation Constant of H_2O, −log K_w, at Saturated Vapor Pressure Calculated Using Eqs. 1–5

T, K*	Vapor	T, K	Vapor	Liquid
273	104.92	598	32.54	11.65
298	95.21	623	26.35	12.12
323	87.13	633	23.38	12.48
348	80.28	638	21.66	12.74
373	74.35	643	19.56	13.18
398	69.09	644	19.03	13.32
423	64.31	645	18.42	13.51
448	59.84	646	17.64	13.81
473	55.55	646.40	17.37	13.93
498	51.32	646.65	17.04	14.07
523	47.04	646.85	16.70	14.24
548	42.58	647.05	16.15	14.61
573	37.82	T_c**	15.34	15.34

*See the footnote of Table 3.
**Critical Temperature (647.126 K).

Table 5. Negative Log (Base 10) of Dissociation Constant of H_2O, −log K_w, in Critical Region Calculated With Eqs. 1–5

	Temperature, K*						
Pres. MPa	633	643	648	653	663	673	693
30	11.78	12.03	12.18	12.37	12.98	14.53	19.40
27.5	11.87	12.16	12.36	12.63	13.92	17.78	21.88
25	11.98	12.34	12.64	13.20	18.74	21.59	24.30
24	12.03	12.44	12.83	14.08	20.80	22.92	25.24
23	12.08	12.57	13.19	19.01	22.52	24.19	26.18
22	12.15	12.77	19.28	21.79	24.04	25.39	27.11
20	12.31	23.27	24.54	25.44	26.74	27.66	28.94
17.5	26.39	27.96	28.52	28.99	29.75	30.34	31.20
15	30.77	31.53	31.84	32.11	32.57	32.93	33.46

*See the footnote of Table 3.

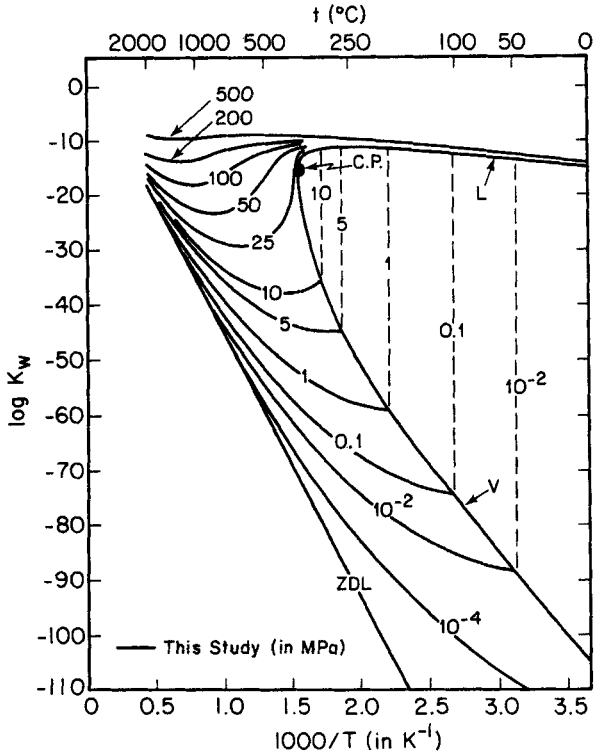

Figure 6. Calculated values of log K_w from Eqs. 1–5 as a function of $10^3/T$ at selected pressures.

ZDL stands for zero density limit. Dashed isobars connect log K_w values for coexisting liquid and vapor.

Uncertainty estimates for our calculated values of log K_h were obtained using the procedures discussed previously (Tanger and Pitzer, 1989). These procedures account for uncertainties in log K_h arising from the uncertainties in the values of ϵ, ΔH_j, and ΔS_j used in Eq. 2. In these uncertainty calculations, we considered the experimental ΔH_j and ΔS_j values for OH^- and H_3O^+ reported by Meot-ner and Speller (1986).

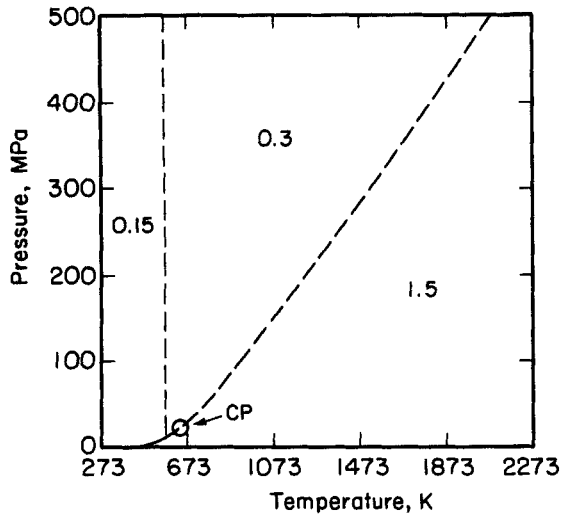

Figure 7. Estimated "average" uncertainties for log K_w values from Eqs. 1–5 in log units for various regions of pressure-temperature.

Initial estimates for the uncertainties in log K_w were taken as the sum of the uncertainties for log K_2 and log K_h. Then, we adjusted our initial uncertainty estimates based on consideration of the observed differences with the experimental data (Figures 2–4 and Table 1). Our final best estimates for the log K_w uncertainties of our model are given as "averages" (in log units) for various pressure-temperature regions as shown in Figure 7. Maximum uncertainties for the P–T regions represented in Figure 7 should be about twice the "average" values.

In principle, the model used here to calculate log K_w should permit calculation of ionization constants for other highly polar fluids. In this paper, we have shown that our model provides reasonable estimates for the ionization constant of H_2O from 273 to 2,273 K and pressures up to 500 MPa.

Acknowledgment

This work was supported by the Director, Office of Energy Research, Office of Basic Energy Sciences, Chemical Sciences Division, of the U.S. Department of Energy under Contract No. DE-AC03-76SF00098. We thank W. L. Marshall and an anonymous referee for their comments.

Notation

$b_1 - b_6$ = coefficients for τ parameter temperature function, Eqs. 5a–b
$d_1 - d_5$ = coefficients for $\bar{V}^*_{H_2O}$ parameter temperature function, Eq. 3
f_{H_2O} = fugacity of H_2O, MPa
G = Gibbs free energy, kJ · mol^{-1}
$\Delta G_1 - \Delta G_4$ = Gibbs free energy changes for steps 1 to 4 of Cycle I
H = enthalpy, kJ · mol^{-1}
K = equilibrium constant
k_2, k_3 = coefficients for $\bar{V}^*_{H_2O}$ parameter pressure function, Eq. A-1
M = mole weight, g · mol^{-1}
MF81 = equation of Marshall and Franck (1981)
n = number of inner shell H_2O molecules, Eq. 2
P = pressure, MPa
P_∞ = infinite pressure
P82 = equation of Pitzer (1982)
R = gas constant
R^*_k = effective electrostatic Born radius for kth electrolyte, Eqs. 2 and 4
r_x = Pauling's crystallographic radius of ion
S = entropy, J · mol^{-1} · K^{-1}
T = temperature, K
t = temperature, °C
$\bar{V}^*_{H_2O}$ = effective molal volume increment per inner shell H_2O molecule of hydration, Eqs. 2 and 3
X = mole fraction
Z = ionic charge

Greek letters

Δ = change in thermodynamic property
δ = difference between calculated and experimental value
ϵ = dielectric constant of H_2O
η = Avogadro's number times elementary charge squared divided by 2
ν = stoichiometric coefficient
ρ = density of H_2O, kg · m^{-3}
τ = ion-independent temperature function, Eqs. 5a–b
ϕ = fugacity coefficient

Superscripts

* = effective quantity
– = molal quantity

Subscripts

aq = hypothetical 1 molar ideal solution standard state
fl = pure fluid standard state
g = hypothetical ideal gas at 1-bar standard state
h = ionic hydration transfer process
j = jth hydration step, Eq. 2
k = *k*th aqueous electrolyte
o = anhydrous gaseous solute species
r = reference conditions for temperature or pressure
w = H_2O

Literature Cited

Ahrens, L. H., "The Use of Ionization Potentials: Part 1. Ionic Radii of the Elements," *Geochim. Cosmochim. Acta*, **2**, 155 (1952).

Arshadi, M., and P. Kebarle, "Hydration of OH^- and O_2^- in the Gas Phase; Comparative Solvation of OH^- by Water and the Hydrogen Halides; Effects of Acidity," *J. Phys. Chem.*, **74**, 1483 (1970).

Chase, Jr., M. W., C. A. Davies, J. R. Downey, Jr., D. J. Frurip, R. A. McDonald, and A. N. Syverud, "JANAF Thermochemical Tables Third Edition," *J. Phys. Chem. Ref. Data*, **14**, Suppl. 1, 1 (1985).

Giguere, P. A., "The Great Fallacy of the H^+ Ion and the True Nature of H_3O^+," *J. Chem. Educ.*, **56**, 571 (1979).

Haar, L., J. Gallagher, and G. Kell, *NBS/NRC Steam Tables: Thermodynamic and Transport Properties and Computer Programs for Vapor and Liquid States of Water in SI Units*, Hemisphere, Washington, DC (1984).

Klots, C. E., "The pH of Steam," *J. Phys. Chem.*, **88**, 4407 (1984).

Kryukov, P. A., L. I. Starostina, and E. G. Larionov, "Ionization of Water at Pressures from 1 to 6000 bar and Temperatures from 25 to 150°C, " *Water and Steam Proc.*, Int. Conf. Prop. Steam, J. Straub and K. Scheffler, eds., Pergamon, New York (1980).

Lau, Y. K., S. Ikuta, and P. Kebarle, "Thermodynamics and Kinetics of the Gas-Phase Reactions: $H_3O^+ (H_2O)_{n-1} + H_2O = H_3O^+ (H_2O)_n$," *J. Am. Chem. Soc.*, **104**, 1462 (1982).

Marcus, Y., "Ionic Radii in Aqueous Solutions," *Chem. Rev.*, **88**, 1475 (1988).

Marshall, W. L., and E. U. Franck, "Ion Product of Water Substance, 0 – 1000°C, 1 – 10,000 Bars. New International Formulation and Its Background," *J. Phys. Chem. Ref. Data*, **10**, 295 (1981).

Meot-ner, M., and C. V. Speller, "Filling of Solvent Shells about Ions: 1. Thermochemical Criteria and the Effects of Isomeric Clusters," *J. Phys. Chem.*, **90**, 6616 (1986).

Payzant, J. D., R. Yamdagni, and P. Kebarle, "Hydration of CN^-, NO_2^- NO_3^-, and OH^- in the Gas Phase," *Can. J. Chem.*, **49**, 3308 (1971).

Pitzer, K. S., "Self-Ionization of Water at High Temperature and the Thermodynamic Properties of the Ions," *J. Phys. Chem.*, **86**, 4704 (1982).

Pitzer, K. S., "Dielectric Constant of Water at Very High Temperature and Pressure," *Proc. Nat. Acad. Sci. USA*, **80**, 4575 (1983).

Quist, A. S., "The Ionization Constant of Water to 800° and 4000 Bars," *J. Phys. Chem.*, **74**, 3396 (1970).

Sweeton, F. H., R. E. Mesmer, and C. F. Baes, Jr., "Acidity Measurements at Elevated Temperatures: VII. Dissociation of Water," *J. Soln. Chem.*, **3**, 191 (1974).

Tanger IV, J. C., and H. C. Helgeson, "Calculation of the Thermodynamic and Transport Properties of Aqueous Species at High Pressures and Temperatures: Revised Equations of State for the Standard Partial Molal Properties of Ions and Electrolytes," *Amer. J. Sci.*, **288**, 19 (1988).

Tanger IV, U. C., and K. S. Pitzer, "Calculation of the Thermodynamic Properties of Aqueous Electrolytes to 1000°C and 5000 Bar from a Semicontinuum Model for Ion Hydration," *J. Phys. Chem.*, **93**, 4941 (1989).

Uematsu, M., and E. U. Franck, "Static Dielectric Constant of Water and Steam," *J. Phys. Chem. Ref. Data*, **9**, 1291 (1980).

Appendix: Revision of the $\bar{V}^*_{H_2O}$ Parameter

In development of the semicontinuum model (Eq. 2), it was assumed that the parameter $\bar{V}^*_{H_2O}$ is independent of pressure. This assumption is consistent with incompressible H_2O molecules in the first hydration shell. However, the discrepancies between the experimental and calculated pressure dependence for log K_w, shown in Figure 4, suggest that inner-shell H_2O molecules have a small, finite compressibility. In order to investigate this compressibility contribution, we allowed $\bar{V}^*_{H_2O}$ to vary with pressure as given by

$$\bar{V}^*_{H_2O(P,T)} = \bar{V}^*_{H_2O(P_\infty,T)} + [k_2/(k_3 + P)], \qquad \text{(A1)}$$

where P_∞ denotes infinite pressure, and k_2 and k_3 are empirical constants.

Equation A1 requires revision of the expression for ϕ_o/ϕ_n in Eq. 2 from $-nP\bar{V}^*_{H_2O}/RT$ to

$$\frac{-n}{RT}\{P\bar{V}^*_{H_2O(P_\infty,T)} + k_2 \ln [(k_3 + P)/k_3]\}. \qquad \text{(A2)}$$

In order to simplify application of Eqs. A1 and A2 at any temperature of interest, we assumed that Eq. 3 could be used to represent $\bar{V}^*_{H_2O(P_\infty,T)}$ if d_1 in Eq. 3 was treated as an adjustable parameter. In addition, we set $r_x(H_3O^+) = r_x(OH^-) = 0.140$ nm, which is consistent with our prior value for OH^- and is also consistent with the $r_x(H_3O^+)$ value given by Marcus (1988). Appropriate revision of Eq. 2 using Eq. A2, as described above, allowed trial-and-error calculation of the "best-fit" values for d_1, k_2 and k_3 which optimized agreement with high-pressure log K_w measurements.

Using the high-pressure log K_w measurements at 298 K shown in Figure A1, we obtained "best-fit" values which yield the solid curve for 298 K. These "best-fit" values of d_1, k_2, and

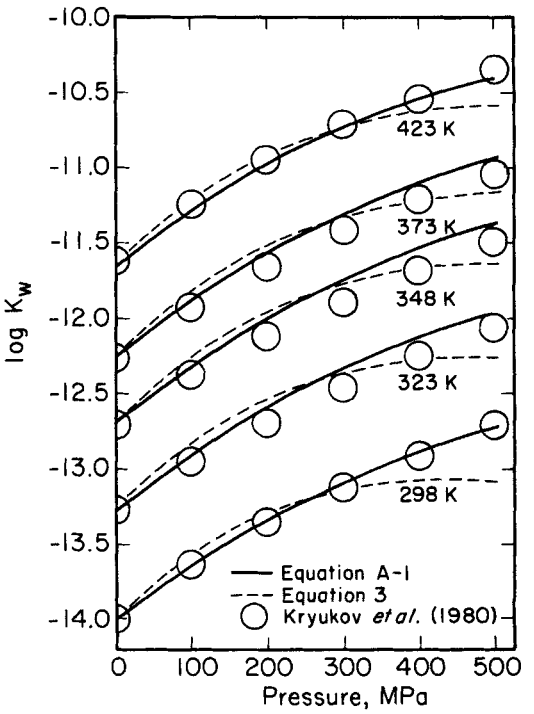

Figure A1. Revised calculated values of log K_w using Eqs. A1 and A2 for selected isotherms as a function of pressure.

k_3 are 16.60 in 10^{-6} m^3 · mol^{-1}, 7.0 × 10^{-4} MPa · m^3 · mol^{-1}, and 250 MPa, respectively. These values were then used to independently predict the solid curves at the other temperatures represented in Figure A1. As can be seen in the figure, the revised $\bar{V}^*_{H_2O}$ model significantly improves the description of log K_w as a function of pressure.

The net effect of a pressure-dependent $\bar{V}^*_{H_2O}$ parameter on calculated values of log K_w decreases to very small values with increasing temperature. Nevertheless, provision for a pressure-dependent $\bar{V}^*_{H_2O}$ parameter is desirable for improving our model at temperatures from 273 to ~473 K. However, revision of the $\bar{V}^*_{H_2O}$ parameter will not be pursued further in this study.

Manuscript received Mar. 3, 1989, and revision received June 23, 1989.

See NAPS document no. 04714 for 3 pages of supplementary material. Order from NAPS c/o Microfiche Publications, P.O. Box 3513, Grand Central Station, New York, NY 10163. Remit in advance in U.S. funds only $7.75 for photocopies or $4.00 for microfiche. Outside the U.S. and Canada, add postage of $4.50 for the first 20 pages and $1.00 for each of 10 pages of material thereafter, $1.50 for microfiche postage.